バイオサイエンス研究科　博士論文要旨

所属 （主指導教官）	細胞構造学講座（塩坂　貞夫）		
氏名	岡　卓也	提出	平成 14 年　2 月　1 日
題目	Cellular and molecular biological analyses of mouse neuropsin （マウスニューロプシンの細胞、分子生物学的解析）		

A serine protease neuropsin expressed in the hippocampus of adult mouse brain has been implicated in synaptic plasticity. Although the expression of neuropsin mRNA achieved to the peak at neonatal stage, however, it remained to be cleared whether neuropsin participate in developmental function in central nervous system. To investigate this possibility, I examined the localization and function of neuropsin in primary hippocampal neuron. Alternatively, although crystal structure of neuropsin provides the clue to the biological activity of neuropsin, e.g. the activity of substrate hydrolysis and the secretory manner, there is no evaluation experimentally. To address this issue, I performed the mutational analyses of neuropsin.

First, it was revealed that endogenous neuropsin was localized extracellularly in neuronal cell bodies and their neurites in mouse hippocampal cultures. Furthermore, I found that, in cultured mouse hippocampal neurons, recombinant neuropsin enhanced neurite projection from soma after 14 hours of culture and neuronal aggregation with neurite fascicles at 48 hours. This suggests that neuropsin is involved in neurite outgrowth and fasciculation during the development of the nervous system.

Second, I described the examination of the several structural features of neuropsin with use of site directed mutagenesis on its activity and regulated secretion from the cell. Neuropsin is a member of the S1 (clan SA) family of serine proteases and forms characteristic surface loops surrounding the substrate-binding site (J Biol Chem 1999, 274:4220-4224). The loops include those stabilized by six disulfide bonds or a loop C (Gly^{69} to Glu^{80}) and an *N*-glycosylated kallikrein loop (His^{91} to Ile^{103}) not containing a site linked by a disulfide bond. Little, however, is known about the roles of these loops. Thus, the present study investigated whether surface loop structures of neuropsin were essential for the generation of enzymatic activity and/or secretion of the enzyme via a regulated secretory pathway. Among the six disulfide bonds, only SS1 in loop E (Gly^{142} to Leu^{155}) and SS6 in loop G (Ser^{185} to Gly^{197}) were necessary for the catalytic efficiency of neuropsin. Disruptions of loop C and the *N*-linked oligosaccharide chain on the kallikrein loop affected the catalytic efficiency and P2-specificity, respectively. Alternatively, disruptions of loop C and the kallikrein loop enhanced the regulated secretion, while, there was no one disruption which inhibited the secretion, indicating that there was no critical loop required for the regulated secretion among loops surrounding the substrate-binding site. The present results provide new information on the structure-function of family S1(clan SA) serine proteases.

博士論文番号：9981006

Cellular and molecular biological analyses of mouse neuropsin

（マウスニューロプシンの細胞、分子生物学的解析）

岡　卓也
奈良先端科学技術大学院大学
バイオサイエンス研究科　細胞構造学講座
（塩坂　貞夫　教授）

平成１４年１月８日提出

Introduction

Several serine proteases have been shown to play important roles in synaptic plasticity (1-3). These functions are suggested to be mediated by the activation of specific cell surface receptors and the degradation of extracellular matrix (ECM) proteins and cell adhesion molecules (4,5). Neuropsin mRNA was found to be expressed in the forebrain limbic area and has been demonstrated to be engaged in activity-dependent plasticity changes in neurons (6). For example, i) injection of antibody against neuropsin significantly ameliorated epileptogenesis in mice (7); and ii) application of recombinant active-neuropsin had a regulatory effect on the Schaffer-collateral long-term potentiation (LTP) in the mouse hippocampus (2). Furthermore, the activity of neuropsin is regulated by a specific inhibitor, serine proteinase inhibitor-3 (SPI3), in adult mouse brain (8). While recent research has been directed at understanding the physiological function of neuropsin concerning synaptic plasticity, there have been few histochemical analyses showing the localization of neuropsin. Therefore I attempted to determine using immunofluorescence histochemistry whether endogenous neuropsin is expressed in hippocampal neurons and, if so, its localization. Neuropsin mRNA is expressed in neurons in the hippocampus of mouse brain from embryonic day 18 to the adult stage (9). The expression at an early stage implies an alternative role for neuropsin in neuronal development, in addition to synaptic plasticity as described above. However, little is known about these phenomena. Therefore, I observed the morphological effect of the application of recombinant neuropsin on cultured hippocampal neurons.

Neuropsin is a secretory serine protease. The crystal structure of neuropsin has a serine protease fold that exhibits chimeric features of trypsin and nerve growth factor-γ (NGF-γ), a member of the kallikrein family (Fig. 4A) (10), both of which are a part of the S1 family (clan SA) of serine proteases (11). All S1 serine proteases possess

two β-barrels with a catalytic His^{57} (chymotrypsin number), Asp^{102}, and Ser^{195} located at the interface of the two domains (11). These proteases, however, show diversity in the structures of surface loops surrounding the substrate-binding site and it has been proposed that this diversity controls the specificity of enzymatic activity (10,12-15). Four to six disulfide bonds form which likely provide a degree of structural rigidity to the loop structures (10,16,17). Neuropsin possesses six disulfide bonds the same as trypsin. Furthermore, neuropsin forms a loop C (Gly^{69} to Glu^{80}) and an *N*-glycosylated loop D (18), the "kallikrein loop" (His^{91} to Ile^{103}), not containing a site linked by a disulfide bond. The loop C of neuropsin has been superimposed on that of trypsin and NGF-γ (10,19,20). On the other hand, the kallikrein loop is present in all members of the kallikrein family but not trypsin. However, the kallikrein loop of neuropsin differs radically from that of NGF-γ and of kallikrein (10,20). While the loop of most members of the kallikrein family is cleaved into highly mobile nicked chains, that of neuropsin is packed without any nicked sites. This three-dimensional view of neuropsin provides the opportunity to examine the correlation between structure and substrate specificity (10) and it is necessary to evaluate the correlation experimentally.

Most family S1 (clan SA) serine proteases are synthesized as precursors and then enter the secretory pathway (11). It has been indicated that some are sorted to a regulated secretory pathway (21-24). For example, the secretion of trypsinogen, elastase, and cathepsin G is clearly regulated (21,22), while it is debatable whether kallikrein is secreted in a regulated manner (25,26). However, it is not known which domain of these proteases is involved in regulated secretion. On the other hand, there is physiological evidence that neuropsin is involved in activity-dependent synaptic plasticity (2,3,6,7). However, it is still not clear whether neuropsin is secreted in response to stimuli. It is, thus, necessary to determine whether a secretagogue causes exocytotic release of neuropsin, and if so, which domain of neuropsin is required for

regulated secretion.

In this context, site-directed removal involving six disulfide bonds, a loop C, and an *N*-glycosylated kallikrein loop of neuropsin was carried out and the effects of these mutations on the enzymatic activity and the regulated secretion were investigated.

Materials and Method

Cell cultures

Primary hippocampal neurons were prepared from 1.5-day-old mice according to a protocol described previously (27). The cells were plated at a density of 600 cells / mm^2 on 0.02% poly-D-lysine (Becton Dickinson Labware, Bedford, MA)-coated glass coverslips in neurobasal medium containing B27 supplement (Life Technologies, Tokyo, Japan) and 0.5 mM glutamine and cultured at 37°C in a 5% CO_2 incubator. The Neuro2a cell line (mouse neuroblastoma; Institute for Fermentation, Osaka, Japan) was grown in Eagle's medium (MEM; Nissui, Tokyo, Japan) supplemented with 1% non-essential amino acids (NEAA) (Life Technologies, Tokyo, Japan) and 10% fetal bovine serum (FBS) at 37°C in a 5% CO_2 incubator. The PC12 cell line (a gift from Dr. Yasuhisa Hukui, University of Tokyo, Japan) was grown in DMEM (Life Technologies) supplemented with 5% FBS and 5% heat-inactivated horse serum (HS) at 37°C in a 10% CO_2 incubator.

RT-PCR

Adult whole hippocampi (ddY mice, 13 weeks old; male) were dissected on silicone (Toshiba Silicone Co., Ltd, Tokkyo, Japan) under a stereoscopic microscope (SMZ-U, Nikon, Tokoy, Japan). Total RNA was isolated by one-step procedure (Chomczynski and Sacchi 1987) using Trizol reagent (Life Technologies) from 2-day- and 7-day-old hippocampal primary cultures (PN-2d and PN-7d) and from mouse hippocampi. Briefly, total RNA (step dilutes 0.1 ~ 100 ng) was reverse transcribed using 100 units MMLV reverse transcriptase (Life Technologies), 200 ng random hexonucleotide primers (Takara Shuzo Co., Ltd, Kyoto, Japan) and 0.5 mM dNTPs (Amersham Pharmacia Biotech, Tokyo, Japan) in buffer supplied by the manufacturer and a reaction volume of 10 µl at 37°C for 1 h. The cDNA synthesized from the total RNA was

amplified for 35 cycles (94°C; 0.5 min, 55°C; 1 min, 72°C; 1.5 min) in a 50-μl reaction mixture containing nested primers (the outside primer pair is listed first): 5'-CCT CTT AGT TCC ACC CTC TT-3'/ 5'-TTC ACG TAG TAT AGT CCG AC -3' and 5'-CTG GAA GGT CGA GAG TGT AT-3'/5'-GTT GGG TCT TCT AGT GTC AG-3' (0.2 μM final concentration), 1.5 mM of $MgCl_2$, 0.2 mM of dNTPs and Taq DNA polymerase (1.25 units; Amersham Pharmacia Biotech) in the buffer supplied with the enzyme in a DNA thermal cycler (Model 9600; Perkin-Elmer Japan Applied Biosystems, Chiba, Japan). The solution containing cDNA products was mixed eith picogreen (Molecular Probes, Inc., Eugene, OR, USA) and subjected to 10% PAGE.

Application of recombinant neuropsin to primary neurons

Recombinant proneuropsin was prepared from a Baculo virus expression system (28) and the buffer containing proneuropsin was changed to a neurobasal medium using an Econopack10DG desalt-column (Bio-Rad, Tokyo, Japan). We measured the amidolytic activity of neuropsin with 50 mM Boc-Val-Pro-Arg-methylcoumarin (Peptide Institute, Inc., Osaka, Japan) (28). One unit was defined as that required to hydrolyze 1 μmol of the substrate per minute at 37°C. The recombinant proneuropsin had low peptidolytic activity (<0.01 U/mg protein). After treatment of proneuropsin with lysyl endopeptidase [EC 3.4.21.50] (Wako Pure Chemical Industries, Ltd., Osaka, Japan) conjugated with Sepharose 4B (Amersham Pharmacia Biotech, Tokyo, Japan) at 37 °C for 50 min, the activity of active-neuropsin was 2.6 U/mg protein. Primary hippocampal neurons were cultured in medium containing recombinant neuropsin, in which there was degradation of neither proneuropsin nor active-neuropsin, for at least 48 hours.

Morphological analysis of primary neurons

At 14, 18, 24 hour cultures, cells were immunostained and the images were captured by

an Axioplan2 (CarlZeiss, Tokyo, Japan). The number of cells, neuritis, and aggregates were counted manually in a 480 x 700 μm square field per experiment.

Plasmid Construction

pED1-NP was constructed as follows. A 789-bp NcoI-XhoI fragment of a full-length neuropsin cDNA was amplified based on NP1-pBluescript(II)KS$^+$ (6) by PCR using the following primers: forward; 5'-CGG GAT ATC ACT CAG CAT AAT G-3' (T7 primer) / reverse; 5'-GGA CTC GAG TCA GTC CCT GTT GTC CAT TGT CTT-3' (primer-A; containing a stop codon and XhoI site), and introduced into the NcoI-XhoI site of pED1 vector (4896-bp) (a gift from Dr. Mahito Nakanishi, Gene Discovery Research Center, AIST, Ibaragi, Japan), which contains the cytomegalovirus enhancer, chicken β-actin promoter (29), and SV40 late polyA signal (30), to generate pED1-NP.

Point mutations were introduced into a full-size neuropsin cDNA of pED1-NP by oligonucleotide-directed mutagenesis using Mutan-Super Express Km according to the manufacturer's protocol (TaKaRa, Siga, Japan). The *numerals* in the clone names indicate the amino acid number counted from the start codon, Met. The following primers were used, and the nucleotides changed relative to the neuropsin cDNA sequence are underlined: C7S, 5'-CCC CCA CCC TCT GCA ATC CA-3'; C39S, 5'-AGG TCG AGA GTC TAT ACC CCA C-3'; C74S, 5'-AGC CCA CTC CAA AAA ACA G-3'; C108S, 5'-GCA TCC TTC CTA CAA CAA C-3'; C145S, 5'-CCA ATC TGT CTC CCA AAG TTG GCC AGA AG -3'; C152S, 5'-TTG GCC AGA AGT CCA TCA TAT CAG G-3'; C198S, 5'-AGG GCA TGG TCT CTG CTG GCA GCA G-3'; C208S, 5'-TGA CAC GTC CCA GGG TG-3'; C233S, 5'-TCA GAC CCC TCT GGG AAA CCC G-3'; C246S, 5'-ACA CCA AAA TCT CCC GCT ACA CTA CC-3'; N110A, 5'-TCC TTG CTA CGC CAA CAG CAA CCC-3'; D206V, 5'-TGG AGC TGT CAC GTG CC-3'; DS211VA, 5'-TGG AGC TGA CAC GTG CCA GGG TGT CGC AGG AGG CCC-3'. Deletion mutants of Δ(S87-P94) and N110S•Δ(N113-E115) were created by PCR with

NP1-pBluescript(II)KS$^+$ (6). PCR-fragments of 250-bp of NcoI-EcoO65I: forward; T7 primer / reverse; 5'-ATG GTC ACC CAG ACG CAC G -3', and 509-bp of EcoO65I-XhoI: forward; 5'-TAC TCC GTG CGT CTG GGT GAC CAT GAG CAG GAG ATC CAG GTG GC-3' / reverse; primer-A, were inserted into the NcoI-XhoI site of pED1 to generate Δ(S87-P94). PCR-fragments of 328-bp of NcoI-NSPV: forward; T7 primer / reverse; 5'-GTT CGA ATA GCA AGG ATG CTG GAT AGA-3', and 446-bp of NSPV-XhoI: forward; 5'-TCT ATC CAG CAT CCT TGC TAT TCG AAC AGC GAT CAC AGT CAC GAT ATA ATG-3' / reverse; primer-A, were inserted into the NcoI-XhoI site of pED1 to generate N110S•Δ(N113-E115). pSIhGH vector encoding human growth hormone was described previously (31).

Transfection

Neuro2a cells were plated at a density of 1.0 X 10^4 / cm^2 (1.0 X 10^5 cells / 35 mm dish) in MEM, 10% FCS, and 1% NEAA on a coverslip (Matsunami, Osaka, Japan) coated with poly-L-lysine (4 μg / cm^2; Sigma, St. Louis, MO). After 18 hours, cells were transfected with 1 μg of pED1-NP and the mutants in OPTI-MEM-1% NEAA by LipofectAMINE PLUS (Life Technologies). After 3 hours, the medium was replaced with fresh OPTI-MEM-1% NEAA containing N-2 supplement (differentiation) (Life Technologies). Conditioned medium (2 ml per 35 mm dish) was recovered after 36 hours of culture for the enzyme assay. PC12 cells were plated at a density of 1.2 X 10^5 / cm^2 (1.2 X 10^6 cells / 35 mm dish) in DMEM, 5% FBS, and 5% HS on a dish coated with polyethylenimine (Sigma). After 18 hours, cells were co-transfected with 1.5 μg of pSIhGH and 1.5 μg of pED1-neuropsin by LipofectAMINE 2000 (Life Technologies). After 48 hours, assays of hGH and neuropsin release were performed.

Immunofluorescence

Primary neurons were placed on ice, treated with or without 0.125% (w/v)

pronase (Calbiochem, Darmstadt, Germany) for 30 min and reacted with rat anti-neuropsin monoclonal antibody (B5mAb 20 mg / ml, Medial and Biological Laboratories, Co., Ltd., Nagano, Japan) (7) in Dulbecco's PBS containing 0.7 mM $CaCl_2$ and 0.5 mM $MgCl_2$ [PBS(+)] on ice for 1h. Then, cells were fixed with 4% paraformaldehyde in PBS(+), reacted with goat anti-rat IgG conjugated with FITC (Jackson Immunoresearch Lab., Inc., West Grove, PA), permeabilized with 0.2% Triton X-100 in PBS, and reacted with rabbit polyclonal antibody against MAP2 (32) (Sigma-aldrich, Tokyo, Japan), a somatodendritic protein of neurons, and goat anti-rabbit IgG conjugated with rhodamine (Biosource International, Camarillo, CA). For the morphological analysis, primary neurons were fixed with 4% paraformaldehyde in PBS(+) and reacted with anti-MAP2 monoclonal antibody (MAB364, Chemicon International Inc., Temecula, CA) or with SMI 31 (anti-phosphorylated neurofilament H, Sternberger Monoclonals Incorporated Alpha Centter, Baltimore, MD) and goat anti-mouse IgG conjugated with FITC (Oregonon Teknika Corporation, Durham, NC).

Neuro2a cells and PC12 cells were fixed with 4% paraformaldehyde in PBS(+) and reacted with the following antibodies: rabbit anti-neuropsin polyclonal antibody (11pAb, 20 μg / ml) (8), rat anti-neuropsin monoclonal antibody (B5mAb, 20 μg / ml), mouse anti-Grp78 monoclonal antibody, (diluted 1:200, StressGen Biotechnologies Corp. Victoria, BC, Canada) (33), rabbit antiserum against α-mannosidase II, a Golgi enzyme, (1:1,000, a gift from Dr. Kelly Moremen, University of Georgia, Athens, GA) (34), and rabbit anti-chromogranin A polyclonal antibody (1:500, a gift from Dr. Seung Hyun Yoo, KAIST, Korea) (35) as primary antibodies; and goat anti-rabbit IgG conjugated with FITC (1:600, Biosource International, Camarillo, CA), goat anti-rat IgG conjugated with rhodamine (1:100, Biosource International), and goat anti-mouse IgG conjugated with FITC (1:600 , Biosource International) as secondary antibodies. Double-labeled immunofluorescence cytochemistry with anti-Grp78, anti-α-mannosidase II, and anti-chromogranin A antibodies was used to observe the

localization of mutant and wild-type neuropsin on the ER (33), Golgi complex (34), and large dense core vesicles (36), respectively.

The coverslips containing immunostained cells were mounted in glycerol containing Mowiol 4-88 (Calbiochem-Novabiochem Corporation, San Diego, CA) and 1,4-diazobicyclo-(2.2.2.)-octane (Sigma-aldrich) (37) and were observed with a Laser scan microscope LSM510 invert (CarlZeiss, Tokyo, Japan).

Quantification of Mutants and Wild-Type Neuropsin in Conditioned Media

Media and cell lysates were subjected to SDS-PAGE using 10% acrylamide gel. The proteins were transferred to a polyvinylidene difluoride (PVDF) membrane (Bio-Rad, Tokyo, Japan). The membrane was reacted with rabbit anti-neuropsin polyclonal antibody (11pAb), and then goat anti-rabbit IgG conjugated with alkaline phosphatase (Bio-Rad) in 5% skim milk in 0.1M Tris-HCl, pH 7.5, 0.15M NaCl, and 0.1% Tween 20. The secondary antibody was detected by enhanced chemiluminescence (Immun-Star Substrate, Bio-Rad), followed by exposure to x-ray film. The amount of mutant and wild-type protein was determined based on the band densities using 1D-gel image analysis software (Quantity One software, PDI, Toyobo Co., Ltd., Osaka, Japan) (8). Recombinant neuropsin (Baculo), purified from a Baculo virus expression system (28), was used as a control of the amount.

For comparison of the activity of 11pAb to bind mutants and wild-type neuropsin, conditioned medium derived from each transfectant was immunoprecipitated with affigel Hz beads (Bio-Rad, Tokyo, Japan) conjugated with F12mAb (7), the beads were subjected to reducing SDS-PAGE, and the band density stained using colloidal properties of Coomassie G-250 (Gelcode blue; PIERCE, Rockford, IL) was compared with the band density obtained by western blotting with 11pAb. There was no difference in the band density of mutants and wild-type neuropsin by western blotting with 11pAb per μg protein contents.

Preparation of Active Neuropsin and Assay of Amidolytic Activity

The amidolytic activity of neuropsin was determined basically as described previously (28). Briefly, conditioned media of Neuro2a cells transfected with mutants and wild type neuropsin were treated with lysyl endopeptidase [EC 3.4.21.50] (Wako Pure Chemical Industries, Ltd., Osaka, Japan) conjugated with Sepharose 4B (Amersham Pharmacia Biotech, Tokyo, Japan) at 37 °C for 15 min and then the amount of mutant and wild-type neuropsin in the medium was determined based on the band density, following reducing SDS-PAGE and immunoblotting. To determine the amidolytic activity, 12.5~200 mM Boc-Val-Pro-Arg-4-methylcoumaryl-7-amide (MCA), Pro-Phe-Arg-MCA, Boc-Phe-Ser-Arg-MCA, and Boc-Asp (Obzl)-Pro-Arg-MCA (Peptide Institute, Inc., Osaka, Japan) were mixed with 50 nM mutant and wild-type neuropsin in 96-well plates (Corning Coster, Tokyo, Japan). The reaction proceeded at 25 °C for 0 to 60 min at 3-min intervals in 50 mM Tris-HCl, pH 8.0, 0.1 mg/ml BSA, and 0.02% NaN_3 and was monitored with a multi-well plate reader (Cytofluor II, PerSeptive Biosystems, Tokyo, Japan). The kinetic parameters *K*m and *k*cat were obtained by linear regression analysis of the Lineweaver-Burk plot.

Depolarization-induced Release

After 48 hours of gene transfection, PC12 cells were washed four times with a low K^+ solution (140 mM NaCl, 4.7 mM KCl, 1.2 mM KH_2PO_4, 2.5 mM $CaCl_2$, 1.2 mM $MgSO_4$, 11 mM glucose, and 15 mM HEPES-NaOH, pH7.4). They were incubated for 2 min with the low K^+ solution and then for 2 min with a high K^+ solution (140 mM NaCl, 59.7 mM KCl, 1.2 mM KH_2PO_4, 2.5 mM $CaCl_2$, 1.2 mM $MgSO_4$, 11 mM glucose and 15 mM HEPES-NaOH, pH7.4), and each medium was recovered. Cell lysates were homogenized in 10 mM HEPES-NaOH, pH 7.4 and 0.2 mM EDTA

using a sonicator (Ultras. Homogenizer, VP-5S, TAITEC, Co., Ltd., Saitama, Japan) and centrifuged at 17,500 xg for 5 min, and then the supernatant was collected. Contents of human growth hormone (hGH) were determined using a hGH ELISA kit (Roche Molecular Biochemicals, Mannheim, Germany) (31). Mutants and wild-type neuropsin were concentrated by acid precipitation with incubation in 6% trichloroacetic acid, 0.0125% deoxycholic acid, and 100 μg / ml gelatin on ice for 1.5 hours and centrifugation at 17,500 xg for 45 min, and then their content was determined by SDS-PAGE followed by western blotting with 11 pAb. Secretion was expressed as a percentage of total cellular hGH, wild-type neuropsin, and the mutants.

Results

Rool of neuropsin in cultured mouse hippocampal neurons

Endogenous neuropsin was distributed on the plasma membrane in cultured neurons.

We detected neuropsin mRNA in primary hippocampal cultures using a semi-quantitative RT-PCR system (38) and found the expression level to be approximately one-tenth of that in adult hippocampus (Fig. 1A), indicating the presence of endogenous neuropsin in primary hippocampal cultures. Thus, immunofluorescence histochemistry was performed to determine the expression pattern of endogenous neuropsin. As recombinant neuropsin is secreted in insect cells transfected with neuropsin cDNA (28), we first investigated whether endogenous neuropsin existed extracellularly in 7 day-old hippocampal primary cultured cells. Cell monolayers were reacted with rat anti-neuropsin monoclonal antibody before the fixation described at materials and methods. Neuropsin signals were detected diffusely on neuronal cell bodies and their neurites extracellularly, whereas MAP2 signals were localized intracellularly (Fig. 1C), and 22 % of neuronal cell bodies among MAP2-positive neurons expressed neuropsin extracellularly (Fig. 1B). To confirm the presence of extracellular neuropsin, cell monolayers were treated with 0.125% (w/v) pronase (Calbiochem, Darmstadt, Germany) for 30 min on ice before being fixed, and then incubated with B5mAb and goat anti-rat IgG conjugated with FITC, resulting in no remaining cell surface-bound neuropsin (Fig. 1B and D). In addition, after pronase-treatment and fixation, cell monolayers were permeabilized and then reacted with B5mAb and goat anti-rat IgG conjugated with FITC. As shown in Fig. 1E, intracellular neuropsin signals were localized as punctate granules in neuronal cell bodies and their neurites. Finally, we indicated histologically that endogenous

neuropsin was expressed and secreted extracellularly in neuronal cells.

Recombinant neuropsin modulates neurite outgrowth and fasciculation of mouse hippocampal neurons in culture

Next, to elucidate the involvement of extracellular neuropsin in neural development, we tested how the application of recombinant neuropsin affected hippocampal cultured neurons. We observed morphological changes of neurons cultured in medium containing active-neuropsin by immunofluorescence histochemistry described at materials and methods (Fig. 2A-H). We found two effects of active-neuropsin on neuronal development: i) neurite projection and ii) neurite fasciculation and cell aggregation. Fig. 2A-C, first, show representative fields at 14 hours in cultures containing active-neuropsin or not. The number of cells having neurites was significantly increased when hippocampal neurons were incubated with active-neuropsin, but not proneuropsin, at 14 and 18 hours culture (Fig. 3A). In addition, application of 2.0 μM active-neuropsin induced an increase of 1.7-fold in the average number of neurites per cell having neurites at 14 hours culture (Fig. 3B). On the other hand, there was no difference in the average length of the longest neurite per cell having neurites at 14 to 24 hours culture (Fig. 3C). It was suggested that active-neuropsin enhances neurite projection specifically. In addition, the activity for neurite projection shown by active-neuropsin was attenuated at 24 hours culture. These results show that active-neuropsin functions only very early in the process of neurite projection.

Second, application of active-neuropsin enhanced cell aggregation and neurite fasciculation at 48 hours (Fig. 2E-H), which was similar to the result observed at 7 days after the start of culture without neuropsin (Fig. 2D). Statistical analysis confirmed that the number of aggregates on addition of 0.8 and 2.0 μM active-neuropsin was increased by 6.1- and 4.2-fold, respectively, while there was no difference in the number of cells per square (Fig. 3D and E). These results suggest that active-neuropsin

facilitates neurite fasciculation and reduces the amount of time required for the aggregation of neurons and fasciculation of neurites.

Finally, the present study shows that neuropsin possesses activity to enhance neurite projection and fasciculation, indicating that extracellular endogenous neuropsin is also involved in these functions locally during neuronal development.

Role of Loop Structures of Neuropsin in Activity of Serine Protease and Regulated Secretion

To investigate the role of the surface loop structure of neuropsin in enzymatic activity and secretion, site-directed mutagenesis was employed in loop C (Gly^{69} to Glu^{80}), the *N*-glycosylated kallikrein loop (His^{91} to Ile^{103}), and six disulfide bonds (Fig. 4B). Neuro2a cells transiently transfected with mutant and wild-type neuropsin cDNA were cultured for 36 hours. Disruption of the disulfide bonds SS2, SS4, and SS5 interrupted the secretion and caused the enzymes to distribute in the ER but not the Golgi complex (Fig. 5). Since the results show quality control of the enzymes, they were uninformative with regard to the enzymatic activity and secretion.

Comparison of Enzymatic Activity between Mutant and Wild-type Neuropsin

Twelve mutants and the wild-type neuropsin had little amidolytic activity without treatment by lysyl endopeptidase (28). Table 1 shows the enzymatic activities of the mutants and wild-type detected after treatment with lysyl endopeptidase.

First, the enzymatic activity was examined with Boc-Val-Pro-Arg-MCA. Mutations in Asp^{189} (D206V; S1 specific pocket) and Ser^{195} (DS211VA; catalytic triad) lacking a protease active pocket resulted in levels of activity ~200- and ~800-fold less than the wild-type as measured by *k*cat/*K*m, respectively (Table 1, lines 3 and 4).

Alternatively, C208S (SS6) and C233S (SS6), had 70~200-fold less activity than the wild-type (Table 1, lines 12 and 13), the *k*cat values being ~200-fold less than and the *K*m values almost the same as the wild-type values. Disruptions of loop C [Δ (S87-P94)] and of a disulfide bond SS1 (C39S) caused hydration of the substrate to occur 22-times more slowly than for the wild-type (Table 1, lines 5 and 10). Both loop C [Δ(S87-P94)] and C39S (SS1) showed a decrease in *k*cat values and increase in *K*m values, indicating that loop C (Gly^{69} to Glu^{80}) and SS1 were necessary for catalytic efficiency. The remaining mutants showed little difference in activity on Boc-Val-Pro-Arg-MCA, relative to the wild-type.

The three-dimensional view has revealed that the kallikrein loop of neuropsin forms a narrow P2 pocket (10). To determine the effect of *N*-glycosylation of the kallikrein loop on the P2-specificity of neuropsin experimentally, the activities of N110A and N110S•Δ(N113-E115) were examined with Pro-Phe-Arg-MCA. Almost the same catalytic activity was found as that of the wild-type in *k*cat/*K*m (Table 1, lines 15-17). However, the *k*cat values were 11- and 4-fold less than that of the wild-type; and *K*m values were 20- and 7-fold lower, indicating enhancement of nonproductive binding of phenylalanine to the S2 site of neuropsin.

The crystal structure indicates that Lys^{175} of loop F is projected toward the S3/S4 site (10) and experimentally, a high level of activity of wild-type neuropsin is observed for synthetic tripeptide substrates having hydrophobic and acidic residues at the P3 position (28). Since the disulfide bond SS3 provides structural rigidity to loop F (Fig. 4A), we determined the effect of SS3 on the P3-specificity of neuropsin, by examining the activity of C145S and C246S (SS3) with Boc-Phe-Ser-Arg-MCA and Boc-Asp (Obzl)-Pro-Arg-MCA. There was no effect on the activities (Table 1, lines 18-20 and 23-25). It was suggested that the disulfide bond SS3 had no effect on the P3-specificity of neuropsin.

Regulated Secretion of Neuropsin

Next, we examined whether wild-type neuropsin could be secreted in a regulated manner. First, we determined the amount of neuropsin secreted after 15 min of exposure to high K^+ medium in Neuro2a cells transfected with wild-type neuropsin cDNA transiently. The result was an increase in the amount by 1.2-fold ($p<0.05$, Student's t-test) relative to that in low K^+ medium (data not shown). This showed that Neuro2a cells secreted low levels of neuropsin in a regulated manner. However, the possibility remained that regulated secretion of neuropsin occurred in an alternate cell line (39,40). Therefore, we next investigated the secretory manner of neuropsin in PC12 cells co-transfected with human growth hormone (hGH) and neuropsin cDNAs transiently. hGH has been well characterized as a regulated secretory protein (41) and the present study also showed that, after 2 min of exposure to high K^+ medium in the presence of calcium, the release of transfected hGH was significantly stimulated 2.5-fold relative to that in low K^+ medium (Fig. 6A). At the same time, we revealed that the release of transfected neuropsin was significantly stimulated by high K^+ medium 3.4-fold and the stimulated secretion was dependent on the presence of calcium (Fig. 6B). Furthermore, immunofluorescence cytochemistry showed that neuropsin distributed as punctate structures in the cytoplasm and neurites of PC12 cells, co-localized with chromogranin A (Fig. 8A arrows). It has been reported that chromogranin A is a major component of large dense core vesicle and plays a key role in regulated secretory granule biogenesis in PC12 cells (36). Thus, the present results are the first evidence that neuropsin was secreted in a regulated manner as well as hGH.

Comparison of the Regulated Secretion of Mutant and Wild-type Neuropsin

To elucidate the roles of each loop of neuropsin in the regulated secretion, the same release assays as employed for the wild-type were performed in PC12 cells transfected with mutant cDNAs (Fig. 7). There was no one disruption which inhibited high K^+-evoked release. Alternatively, high K^+-evoked releases of

high K^+-evoked release. Alternatively, high K^+-evoked releases of three mutants involving loop C [Δ(S87-P94)] and loop D containing an *N*-linked oligosaccharide chain [N110A and N110S•Δ (N113-E115)] were significantly enhanced to 1.6-, 1.7-, and 2.0-fold relative that of the wild-type (Fig. 7 stars). All mutant proteins, except those with disrupted disulfide bonds SS2, SS4, and SS5, co-localized with chromogranin A in cytoplasm and neurites like the wild-type, suggesting that no mutants were excluded from the regulated secretory pathway (Fig. 8 B-E). We conclude that there was no surface loops essential for targeting to the regulated secretory pathway among loops disrupted in the present study.

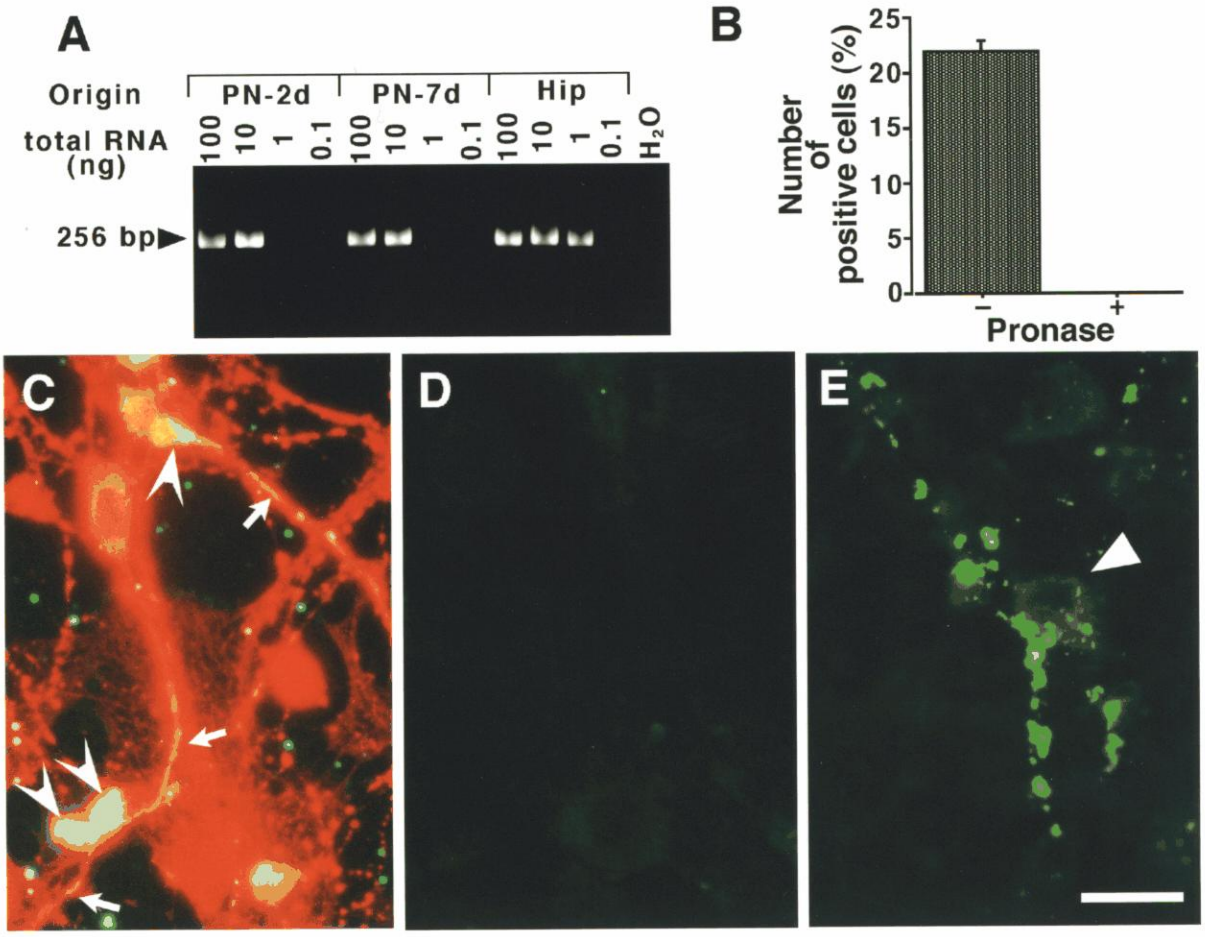

Fig. 1. Expression of neuropsin in mouse primary hippocampal cultures.
A, The patterns of expression revealed by semi-quantitative RT-PCR using nested primers (the outside primer pair is listed first): 5'-CCT CTT AGT TCC ACC CTC TT-3'/ 5'-CAG CCT GAT ATG ATG CAC TT -3' and 5'-CTG GAA GGT CGA GAG TGT AT-3'/5'-GTT GGG TCT TCT AGT GTC AG-3'. Total RNA was isolated from 2-day- and 7-day-old hippocampal primary cultures (PN-2d and PN-7d) and from mouse (ddy males, 13 weeks of age) hippocampus (Hip). PCR products representing neuropsin transcripts (256 bp) but not genomic DNA (538 bp) were present in hippocampal culture and hippocampus *in vivo*. B, % neurons having neuropsin signals extracellularly. Neuronal cell bodies with neuropsin and/or MAP2 signals within ~3.36 x 105 mm2 (three sections of a 480 μm x 700 μm square field per experiment) were measured manually. Error bars show the standard error of five experiments. C, Extracellular periplasmic localization of endogenous neuropsin. A representative field for analysis of (B). Yellow shows neuropsin signals on neuronal cell bodies (arrowheads) and their neurites (arrow) containing MAP2 signals (red). D, Removal of extracellular neuropsin signals by pronase treatment of the cell monolayer. E, Intracellular localization of endogenous neuropsin (green). Bar=20 μm in the inlet of B and E; 200 μm in E.

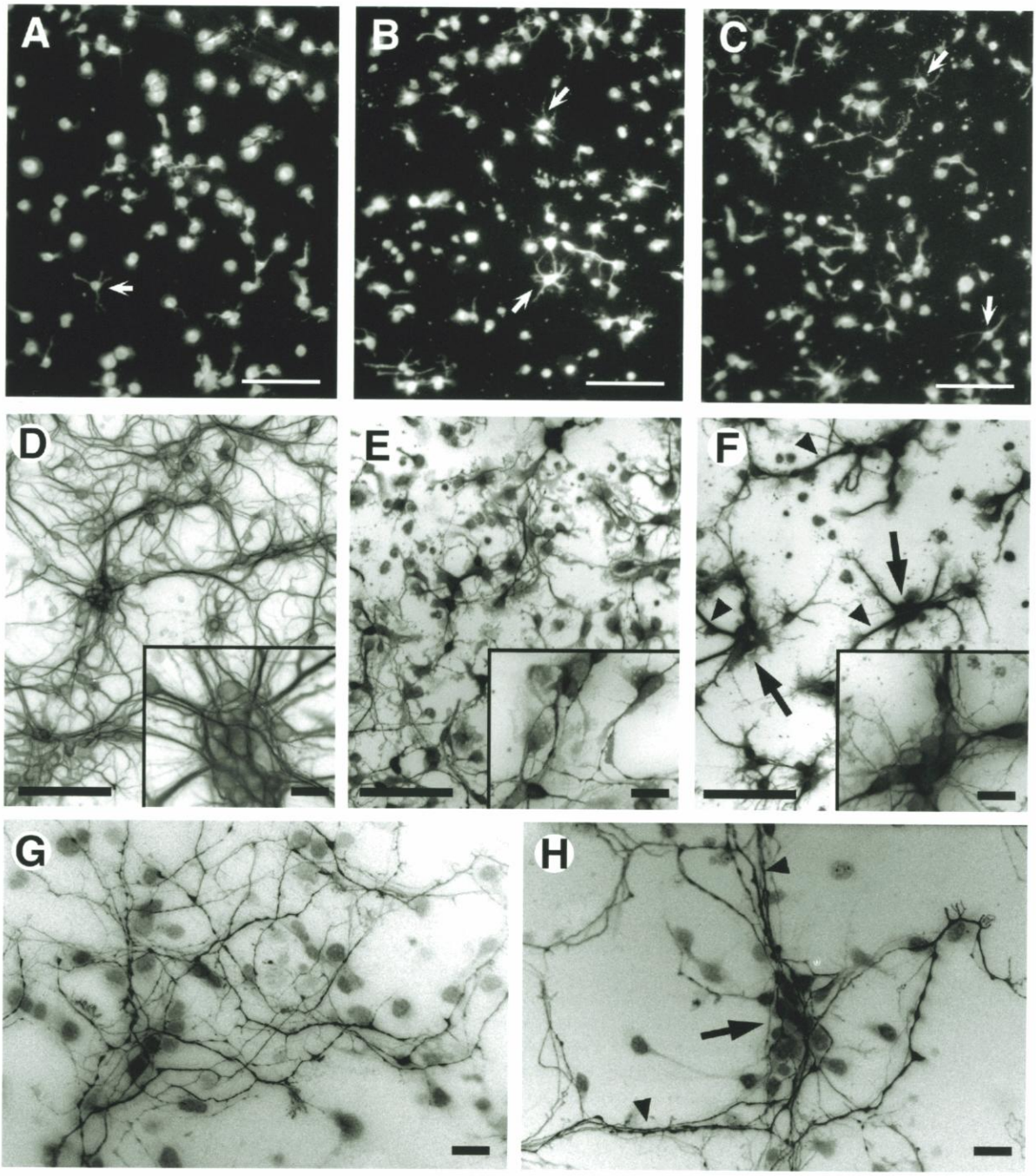

Fig. 2. Effect of recombinant neuropsin on neurite outgrowth, cell aggregation, and neurite fasciculation in cultured hippocampal neurons. Representative immunofluorescence micrographs with anti-MAP2 antibody (A-F) or with SMI 31 (G, H). At 14 hours culture without neuropsin (A); with 0.8 μM active-neuropsin (B); with 2.0 μM active-neuropsin (C). Arrows, neurons having neurites. D, Immunofluorescence micrograph with anti-MAP2 antibody which is showing neurite fasciculation and cell aggregation achieved in 7-day-culture. At 48 hours culture without neuropsin (E); with 0.8 μM active-neuropsin (F). Large arrows, cell aggregates; arrowheads, bundle formation of neurites. Bar=100 μm in A-C; 200 μm in D-F; 20 μm in the inlets of D-F and in G, H. Images are of a negative (D-H).

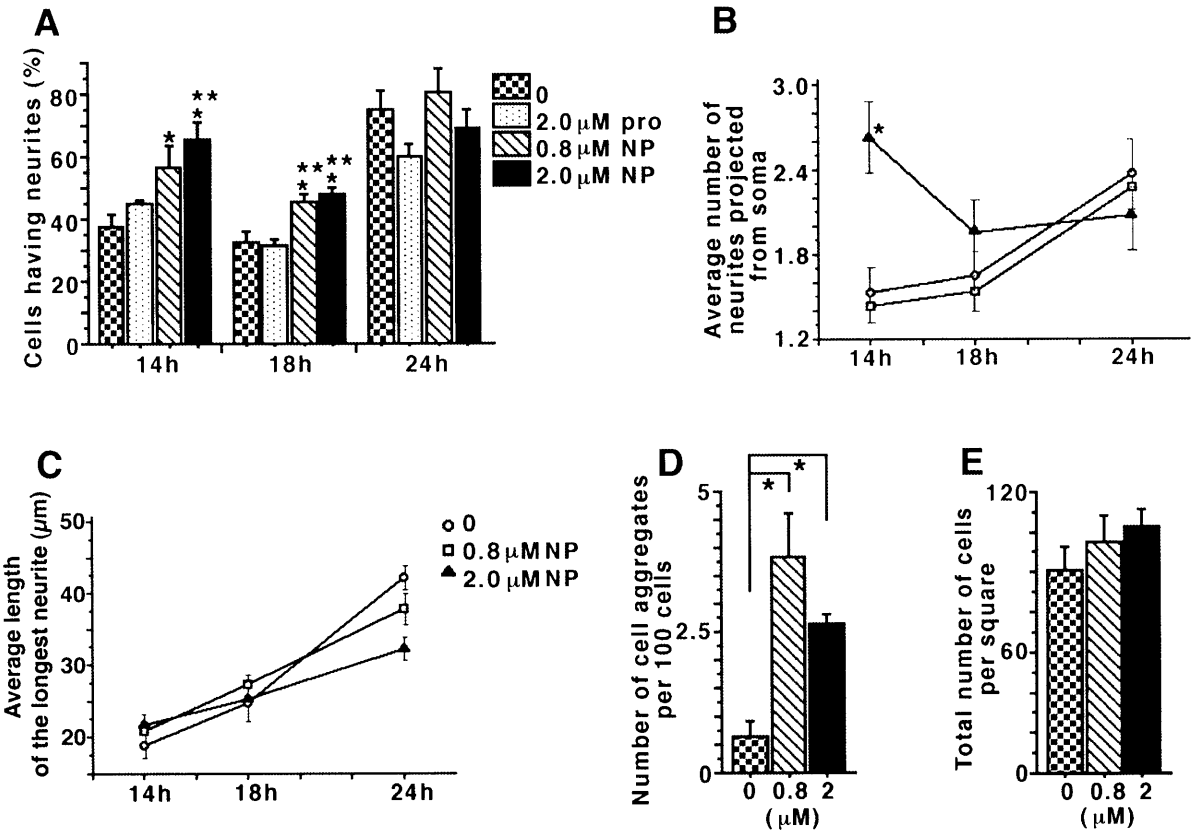

Fig. 3. Statistical analyses of the effect of recombinant neuropsin in cultured hippocampal neurons. A, % neurons having neurites. pro, proneuropsin; NP, active-neuropsin. The number of neurons w/o neurites more than 5 μm in length at 14, 18, and 24 hours culture was counted manually in a 480 μm x 700 μm square field per experiment. Asterisks show statistical significance against that without neuropsin (*) and with 2 μM proneuropsin (**) as determined by one-way ANOVA followed by Fisher' PLSD test for multiple comparisons [$F(3,8)=6.497$, $p=0.0155$ at 14 hours; $F(3,8)=9.469$, $p=0.0052$ at 18 hours; $F(3,8)=2.098$, $p=0.1789$ at 24 hours]. B, Average number of neurites per neuron having neurites in a 480 μm x 700 μm square field. Asterisks show statistical significance against that without neuropsin [$F(2,121)=12.071$, $p<0.0001$ at 14 hours; $F(2,126)=1.462$, $p=0.2356$ at 18 hours; $F(3,113)=0.353$, $p=0.7035$ at 24 hours]. C, Average length of the longest neurites per cell having neurites at 14 to 24 hours culture. There was no significant differences between proneuropsin and active-neuropsin. D, Effect of active-neuropsin on the number of cell aggregates per 100 cells at 48 hours culture. The number of cell aggregates composed of more than 6 cells in circles 40 μm in diameter was counted manually in a 480 μm x 700 μm square field per experiment. Asterisks show statistical significance against that without neuropsin as determined by one-way ANOVA followed by Fisher' PLSD test for multiple comparisons [$F(2,12)=10.636$, $p=0.0022$]. E, No difference in the total number of neurons at 48 hours cultures in a 480 μm x 700 μm square field [one-way ANOVA, $F(2,12)=0.968$, $p=0.4075$]. Error bars show the standard error of three or five experiments (F and G or H and I).

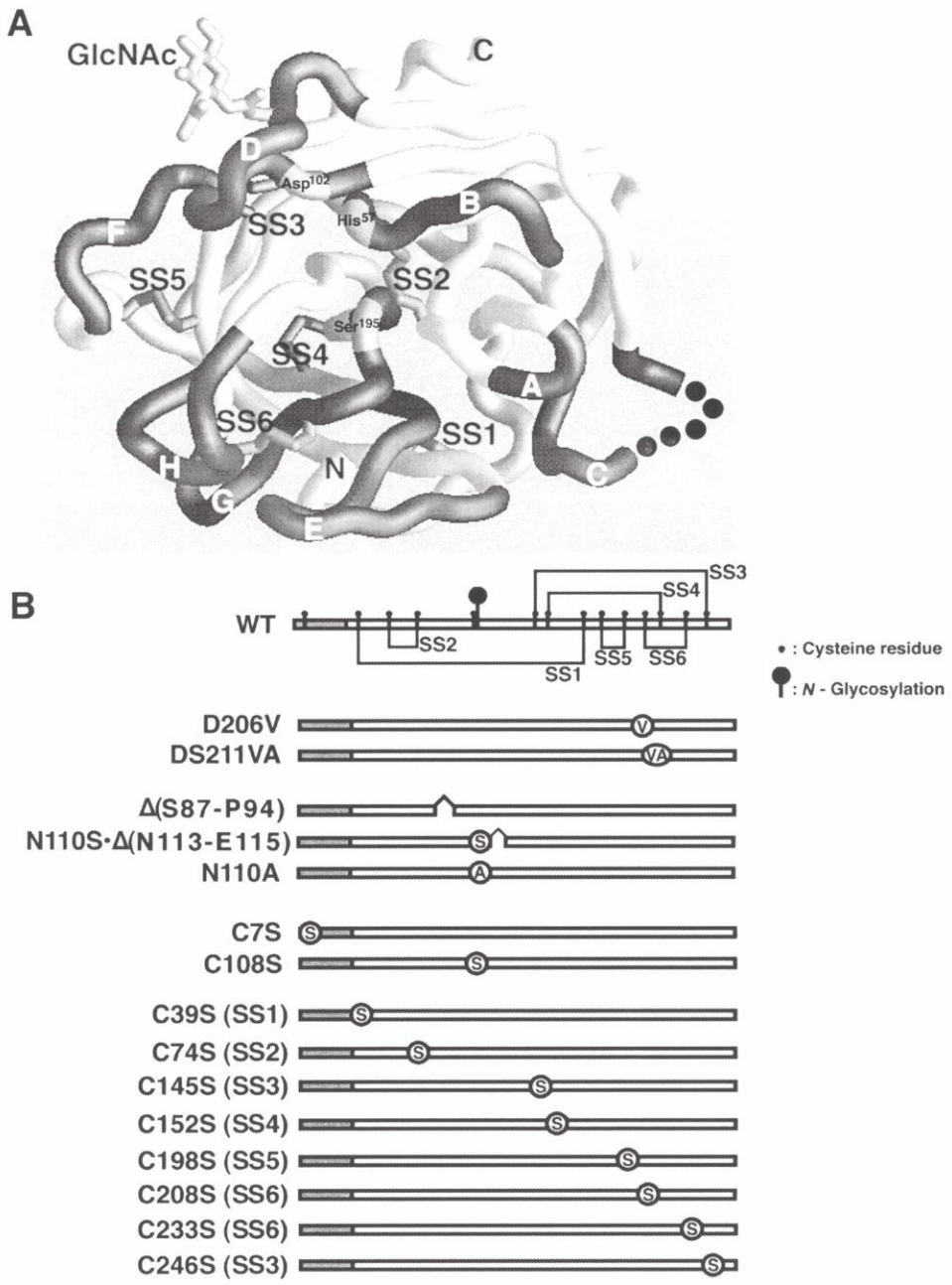

Fig. 4. Structure of mutant and wild-type neuropsin. A, Overall structure of neuropsin (PDB, *code 1NPM*) (9). Note that the *N*-glycosylated loop D is the "kallikrein loop" preserved among the kallikrein family. Catalytic triad, His57 (chymotrypsin number), Asp102, and Ser195; loop structures, A-H (white characters); N- and C-terminals, N and C (black characters); disulfide bonds, SS1-SS6. B, Schematic representation of neuropsin and the established mutations. At the top, the *N*-glycosylation site (large lollipop symbol), two free cysteines (small closed circles) and six disulfide-bonds, SS1-SS6, are indicated (WT, wild-type neuropsin). The ER signal sequence is marked with hatched boxes. The *numerals* in the clone names indicate the amino acid number counted from the start codon, Met. To obtain mutants disrupted at the protease active pocket, Ala or Val was substituted for Asp189 at the S1-specific pocket (D206V) and for Asp194 and Ser195 in the catalytic triad (DS211VA). A deletion of Ser72-Pro79 at loop C was performed [Δ(S87-P94)]. In the *N*-glycosylated kallikrein loop, Asn95, the glycosylation site, was changed to Ala (N110A) and the three amino acids Asn to Glu97 were deleted in addition to substitution of Asn95 with Ser [N110S•Δ(N113-E115)]. Ser was substituted for free cysteine residues (C7S and C108S) and for Cys22 (SS1), Cys58 (SS2), Cys128 (SS3), Cys136 (SS4), Cys182 (SS5), Cys191 (SS6), Cys220 (SS6), and Cys232 (SS3) to disrupt the disulfide bonds (C39S, C74S, C145S, C152S, C198S, C208S, C233S, and C246S).

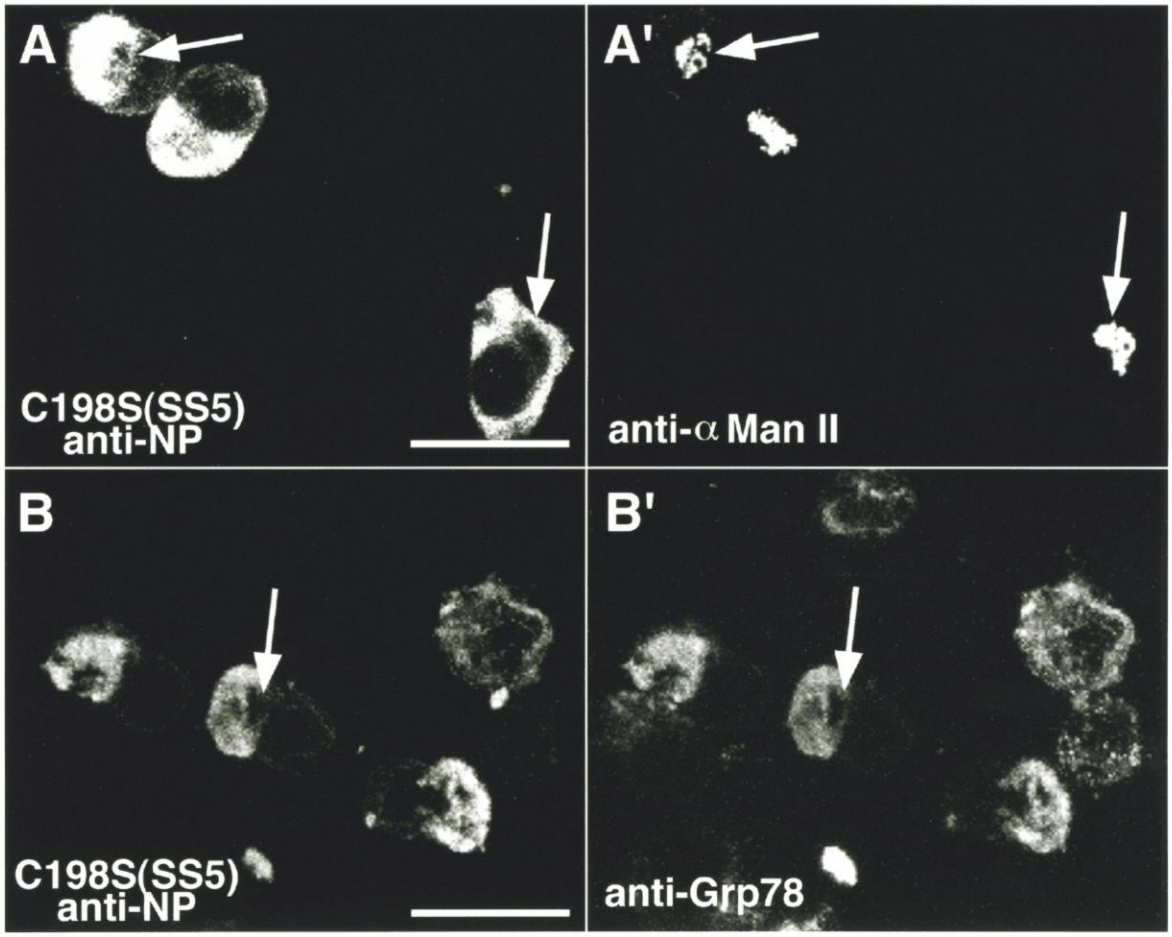

Fig. 5. Immunocytochemical localization of mutant neuropsin in transiently transfected Neuro2a cells. C198S (SS5) cDNA was transiently transfected to Neuro2a and thirty six hours after transfection, cells were processed for double immunofluorescence with the anti-neuropsin (A, B) and anti a-mannosidase II (A') or anti-Grp78 (B') antibodies as described under "Experimental Procedures". Note that C198S (SS5) signals were arrested in ER but not colocalized in Golgi complex (arrows) (A and B). Images for each mutant shown are representative of 3 different experiments. Bar = 20 μm.

Table 1. Enzymatic activity of mutants and wild-type of neuropsin in media of transfected neuro2a cells.

	*k*cat [s^{-1}]	*K*m [μM]	*k*cat / *K*m [$M^{-1}s^{-1}$]
	Boc-Val-Pro-Arg-MCA		
Neuropsin (Baculo)	68.8	245	$2.81x10^5$
WT	100	282	$3.55x10^5$
D206V	0.141	81.9	$1.72x10^3$
DS211VA	0.0387	86.3	$4.48x10^2$
Δ(S87-P94)	15.8	966	$1.64x10^4$
N110S•Δ(N113-E115)	51.6	97.1	$5.32x10^5$
N110A	45.0	152	$2.96x10^5$
C7S	47.0	190	$2.48x10^5$
C108S	78.3	158	$4.95x10^5$
C39S(SS1)	11.6	703	$1.65x10^4$
C145S(SS3)	50.8	110	$4.60x10^5$
C208S(SS6)	0.513	102	$5.03x10^3$
C233S(SS6)	0.424	212	$2.00x10^3$
C246S(SS3)	28.8	119	$2.43x10^5$
	Pro-Phe-Arg-MCA		
WT	193	8360	$2.31x10^4$
N110S•Δ(N113-E115)	49.9	1270	$3.92x10^4$
N110A	18.3	410	$4.47x10^4$
	Boc-Phe-Ser-Arg-MCA		
WT	34.8	216	$1.61x10^5$
C145S(SS3)	38.1	209	$1.82x10^5$
C246S(SS3)	31.4	238	$1.32x10^5$
N110S•Δ(N113-E115)	35.7	215	$1.66x10^5$
N110A	24.5	180	$1.36x10^5$
	Boc-Asp(OBzl)-Pro-Arg-MCA		
WT	31.3	316	$9.92x10^4$
C145S(SS3)	33.1	309	$1.07x10^5$
C246S(SS3)	22.7	287	$7.90x10^4$

Fluorogenic substrate Boc-Val-Pro-Arg-MCA was hydrolyzed in 50 mM Tris-HCl, pH 8.0, 0.1 mg/ml BSA, and 0.02% NaN_3 at 25°C. Representative values for three independent Neuro2a cell transfection experiments were given as averages of triplicate assays.

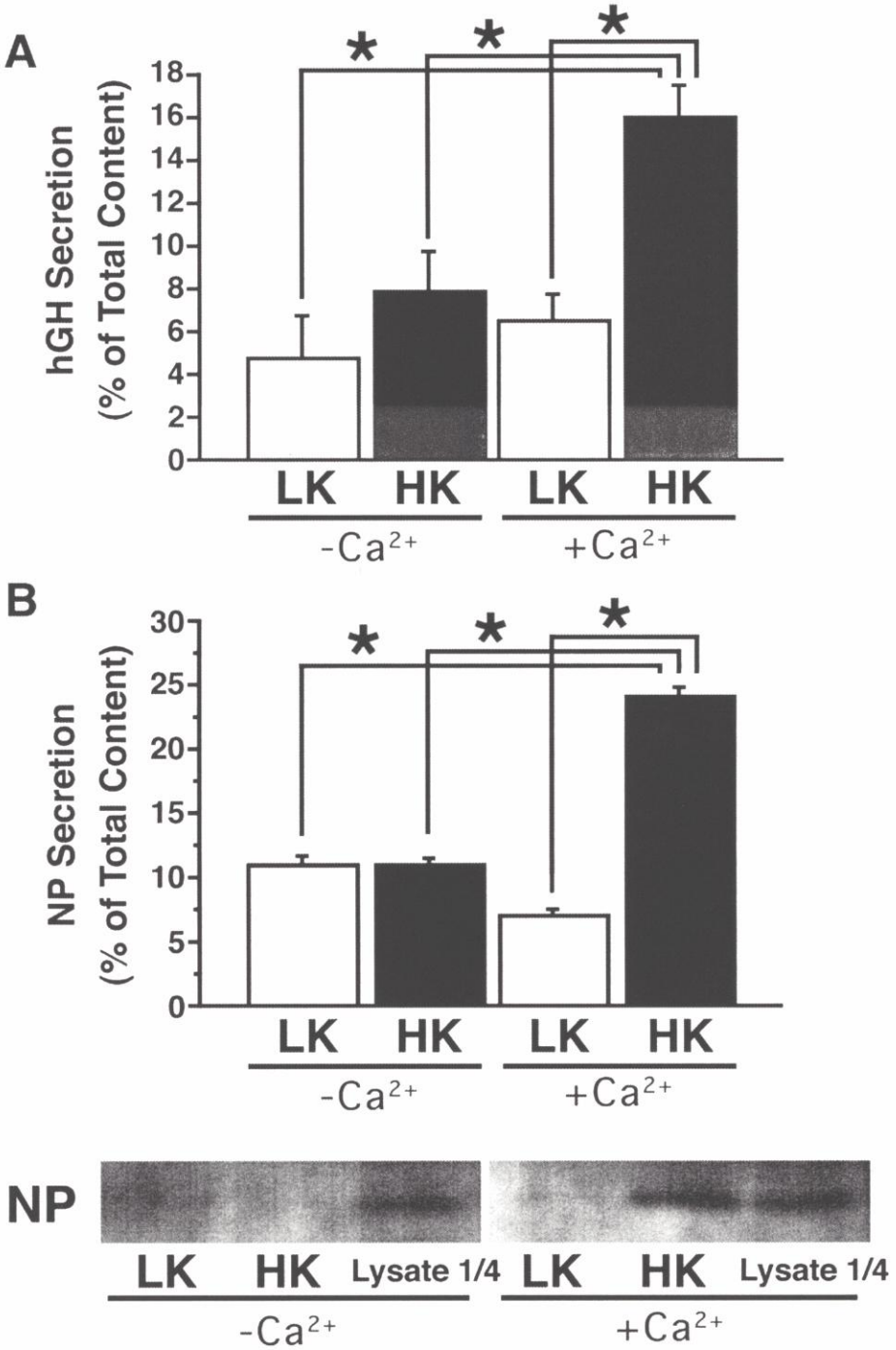

Fig. 6. Ca_{2+} and depolarization-dependent release of neuropsin from neuropsin-transfected PC12 cells. PC12 cells were co-transfected with pSIhGH and pED1-NP. Forty eight hours after transfection, hGH and neuropsin releases were assayed in either low K+ (LK, 4.7 mM KCl) or high K+ solution (HK, 59.7 mM KCl), in the presence or absence of 2.5 mM Ca_{2+}. The amounts of released hGH and neuropsin were expressed as a percentage of the cellular content. Error bars show the standard error of three independent experiments. A, High K+ dependent hGH release. Stars show statistical significance against $+Ca_{2+}$/HK as determined by one-way ANOVA followed by a Bonferroni/Dunn test for multiple comparisons [$F(3, 16)=8.4287$, $p<0.002$]. B, High K+ dependent neuropsin (NP) release. Stars show statistical significance against $+Ca_{2+}$/HK as determined by one-way ANOVA followed by a Bonferroni/Dunn test for multiple comparisons [$F(1, 6)=36.4651$, $p<0.001$]. At the bottom, representative bands of neuropsin are shown. Neuropsin in HK and LK media and 1/4 volumes of cell lysates were run on SDS-PAGE and western blotted with 11pAb.

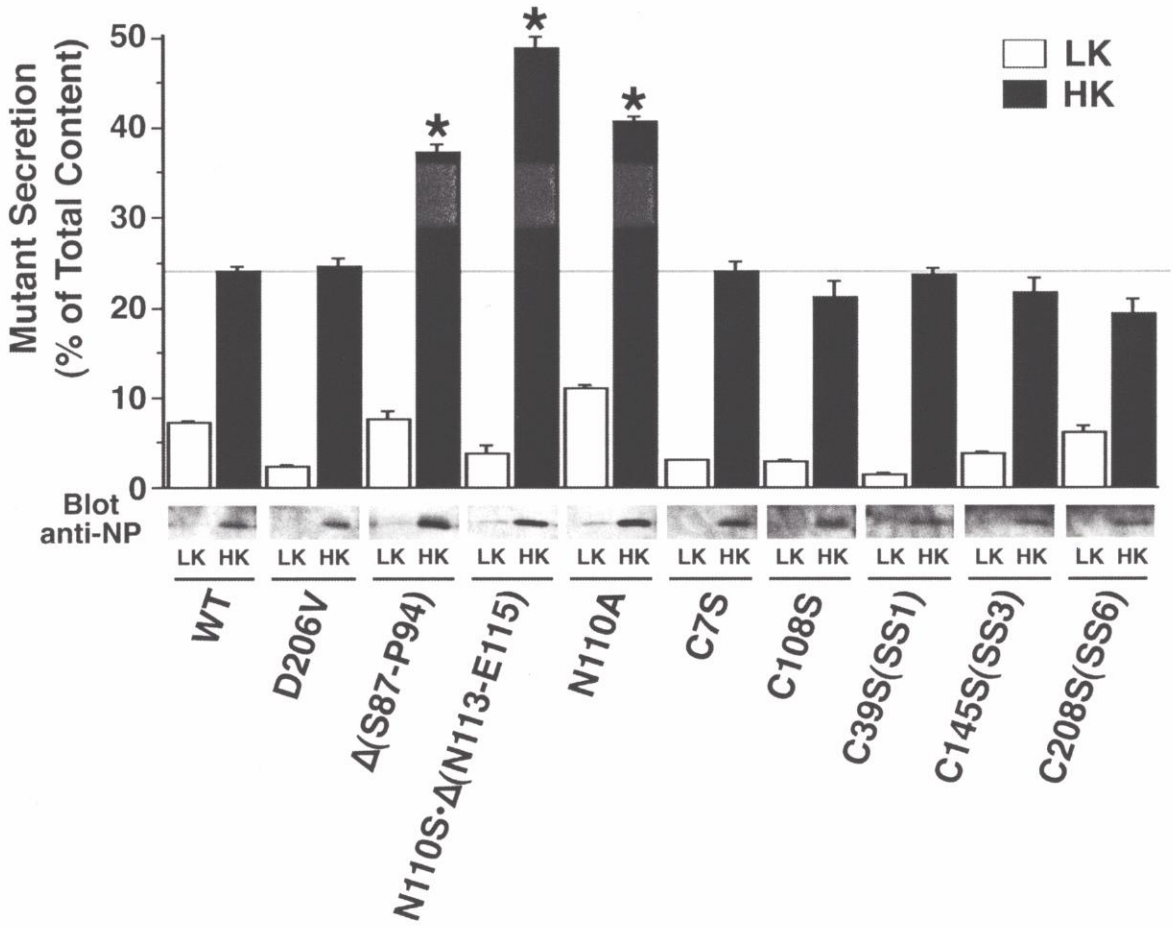

Fig. 7. Comparison of high K+ dependent release between mutant and wild-type neuropsin. PC12 cells were transfected with pED1-mutants or pED1-NP. Forty eight hours after transfection, releases of mutant and wild-type neuropsin were assayed in either low K+ or high K+ solution, in the presence of Ca_{2+}. Percentages of release of wild-type are as in FIG. 6 B. Error bars show the standard error of three independent experiments. Stars show statistical significance against % release of wild-type as determined by one-way ANOVA followed by a Bonferroni/Dunn test for multiple comparisons [$F(9, 28)=75.7756$, $p<0.0001$]. Note that high K+ dependent releases of Δ(S87-P94), N110A, and N110S•Δ(N113-E115) were more inducible than that of wild-type. At the bottom, representative bands of mutant and wild-type neuropsin subjected to SDS-PAGE and western blotting with 11pAb are shown.

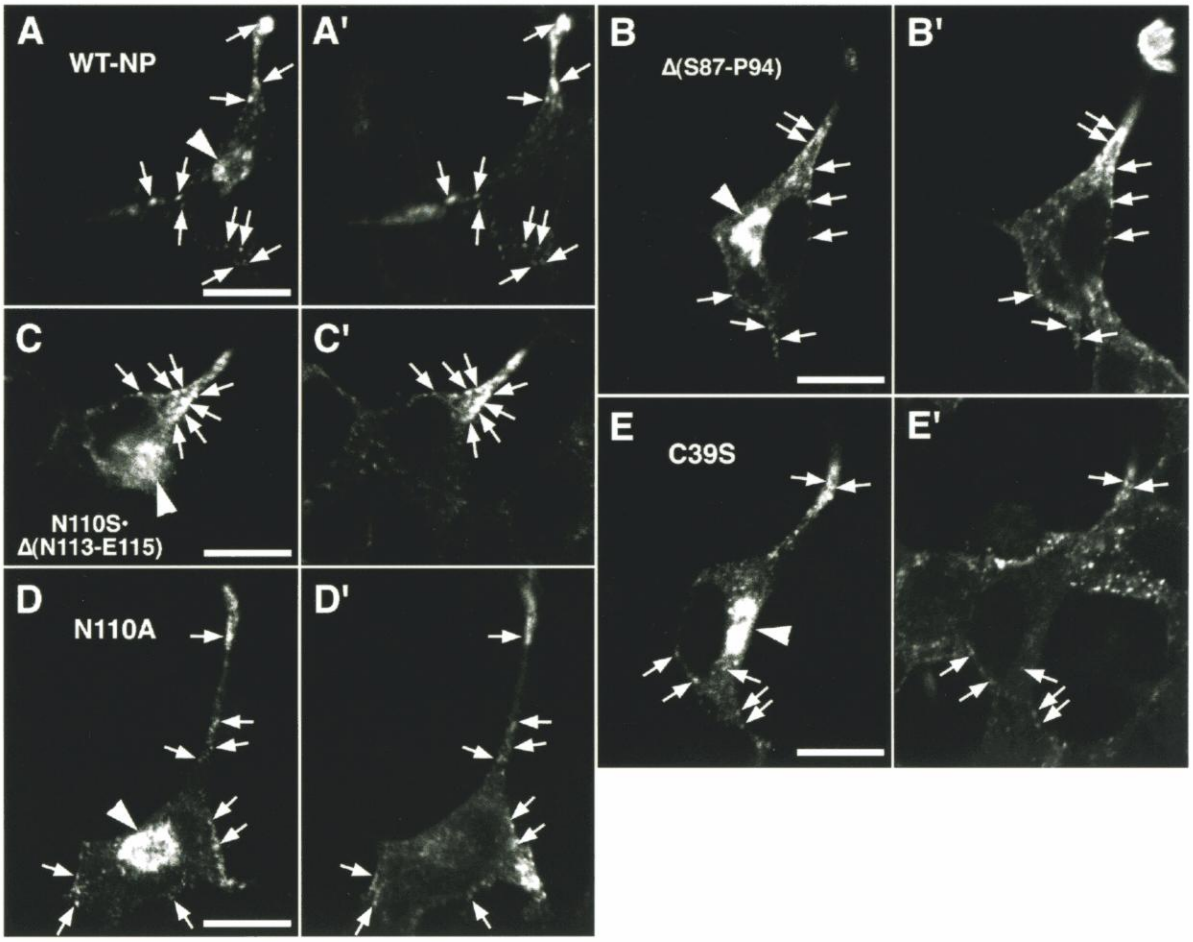

Fig. 8. Co-localization of mutant and wild-type neuropsin with chromogranin A (CGA) in PC12 cells. Double-labeled immunofluorescence cytochemistry with anti-neuropsin (B5mAb) (A-E) and rabbit anti-chromogranin A (A'-E') antibodies. PC12 cells transfected with wild-type or mutant neuropsin [AA', WT-NP; BB', Δ(S87-P94); CC', N110A; DD', N110S•Δ(N113-E115); EE', C39S]. Note that mutants and wild-type neuropsin signals localized as punctate structures in cell bodies and their neurites, where chromogranin A signals co-localized (arrows). Neuropsin signals in Golgi complex determined by double-labeled immunofluorescence as described in "Experimental Procedures" (arrowheads). Bar = 10 μm.

Discussion

Rool of neuropsin in cultured mouse hippocampal neurons

How the secreted neuropsin was associated to the cell surfaces

In this study, It was indicated that endogenous neuropsin was located on cell surface in cultured hippocampal neurons, although there was no transmembrane-spanning region within the neuropsin structures (10). Since there is evidence that neuropsin acts to degrade ECM protein, fibronectin (28), and the cell adhesion molecule, L1, *in vitro* (Matsumoto-miyai, K., et al., in preparation), after secretion, the extracellular periplasmic localization of neuropsin might be attributable to the binding of neuropsin to cell surface molecules including L1 and fibronectin bound to integrin.

How the secreted neuropsin acts in neurite outgrowth, fasciculation and cell aggregation

Recently, it has been proposed that endogenous substrates for an active neuropsin were the extracellular matrix molecule fibronectin (28, 42) and the cell adhesion molecule L1 (Matsumoto-miyai, K., et al., in preparation). Previous reports have shown that fibronectin promoted outgrowth of retinal neurons and the neural Ig superfamily member F11/contactin enhanced the fibronectin-induced outgrowth (43). It was already known that L1 mediates neurite outgrowth, adhesion, and fasciculation during neuronal development (44,45) and as a functional mechanism, dynamin-mediated endocytosis of L1 is necessary for MAPK-dependent neurite outgrowth (46). Alternatively, recent studies have provided evidence that fragments of fibronectin and L1 could also support cell adhesion and migration of tumor cells (47,48). Notably, the release of L1 in tumor cells is mediated by a member of the ADAM metalloproteinase family and the L1 that interacts with neurocan can serve as substrate for integrin-

mediated adhesion and migration (47). In the hippocampus, neuropsin might play a role in the production of soluble L1 instead of the metalloproteinase. In addition, previous study has shown that L1 and fibronectin are found in all regions of the central nervous system (49), suggesting that addition of recombinant active-neuropsin also affects neocortical cultured neurons as well as hippocampal neurons. Finally, neuropsin might modulate neurite outgrowth and fasciculation via fragmentation of fibronectin and L1 in the hippocampus where neuropsin is expressed.

Role of Loop Structures of Neuropsin in Activity of Serine Protease and Regulated Secretion

Effects of mutations on enzymatic activity of neuropsin

The present study provides experimental evidence that characteristic surface loops of neuropsin control the specificity of enzymatic activity.

I. Mutations affecting the P1 specificity of enzyme– Asp^{189} in the S1-specific pocket (D206V) and Ser^{195} in the catalytic triad (DS211VA) were necessary for the catalytic efficiency of neuropsin (Table 1) as well as trypsin (14,50), and disruption of the disulfide bond SS6 resulted in a remarkable reduction in the enzymatic activity of neuropsin. The crystal structure of neuropsin shows that SS6 provides stability in loop G (Ser^{185} to Gly^{197}) (Fig. 4A) (10). And, it was elucidated experimentally that disruption of SS6 induced displacement of loop G and led to a change in the position of Ser^{195}, part of the catalytic triad, resulting in a decrease of enzymatic activity. Since all S1 (clan SA) serine proteases possess SS6, it was proposed that the role of SS6 was common to all the members.

II. Mutations affecting association of enzyme with the C-terminal side of substrate– Known structures of family S1 (clan SA) serine proteases indicate that a loop structure similar to loop E (Gly^{142} to Leu^{155}) of neuropsin, which is stabilized by

the disulfide bond SS1 (Fig. 4A) (10), is in contact with the substrate on the C-terminal side (14). In addition, loop C (Gly^{69} to Glu^{80}) of neuropsin is positioned close to loop E (10,19,20). The effect of loops C and E on catalytic efficiency indicates that interaction of the enzyme with the extended substrate generally helps to maintain catalytic efficiency. On the other hand, a previous report has shown that the loop structure of trypsin similar to loop C of neuropsin contains a calcium binding site and is involved in autolysis, but not enzymatic activity (19,51). Thus, the possibility remains that the effect of the loop C of neuropsin on catalytic efficiency is specific for neuropsin.

III. Mutations affecting the P2 specificity of enzyme– The three-dimensional view has indicated that the kallikrein loop structure (His^{91} to Ile^{103}) of neuropsin affects the S2 site (Fig. 4A) (10). In the present study, it was indeed shown that *N*-linked oligosaccharides on the kallikrein loop affected the size of the P2 pocket. Additionally, N110A was more effective against P2-specificity than was N110A•Δ(N113-E115). The crystal structure indicates that Glu^{97} is projected from the surface to the S1 pocket. Thus, deletion of only *N*-linked oligosaccharides might also affect the projection of Glu^{97}, resulting in an increase of nonproductive binding. Alternatively, since the kallikrein loop of neuropsin differs radically from other members of the kallikrein family as already mentioned (10,20), the present effect of *N*-linked oligosaccharides on P2-specificity might be only specific for neuropsin.

Effects of mutations on regulated secretion of neuropsin

The present results indicated that neuropsin was secreted in a regulated manner. A previous study suggested that a prosegment cleavage event at a dibasic site of an aspartyl protease, prorenin, by proprotein convertases is implicated in the regulated secretion of renin (52). Alternatively, in family S1 (clan SA) serine proteases, previous studies have indicated that the prosegment of neither trypsinogen nor cathepsin G is essential for sorting to the regulated secretory pathway (21,24). Therefore, the

possibility has remained that a site other than the prosegment is relevant for sorting in the regulated manner. The present study investigated effects of disruptions in loop structures of neuropsin on the regulated secretion, and showed that no one critical loop is required for the secretion. Among the loops, loop C and the *N*-linked oligosaccharide chain on the kallikrein loop, however, enhanced the secretion, proposing any involvement of these sites in the secretion.

Concerning several prohormone and proprotein convertases, the amphipathic helical segments are essential for regulated secretion, disruptions causing a severe reduction in the secretion (53-58). Regarding neuropsin, the only candidate for the amphipathic helical loop among the surface loops that surround the substrate-binding site is loop E (10). In the present study, disruption of loop E, however, caused no reduction in regulated secretion, while the effect of the disruption on catalytic efficiency confirms perturbation of the loop E structure. On the other hand, the present study indicated that disruption of loop C caused a significant enhancement of regulated secretion, while no experiments have shown, so far, disruptions to any molelcules that cause an increase in regulated secretion (21,53,54,57,58). Loop C consists of hydrophilic amino acids and is projected to the surface (10) and the functional significance of the increase could not been elucidated in the present study. Thus, it is first necessary to determine whether the increase is common to other S1 (clan SA) serine proteases.

In addition, site-directed removal of the *N*-glycosylation site of neuropsin also enhanced the regulated secretion. The experiments on enzymatic activity confirmed that *N*-linked oligosaccharides provide structural rigidity to the kallikrein loop, which determines the size of the P2 pocket. Thus, changes in the kallikrein loop structure caused by the removal of *N*-linked oligosaccharides might also induce an enhancement of secretion. On the other hand, previous reports have shown that appropriate glycosylation of a number of proteins is important for proper expression and function,

i.e., stability, folding in the ER, trafficking to the Golgi complex and plasma membrane, and catalytic activity (59-67). It remains, therefore, possible that variability among sugar structures in the kallikrein loop affects the regulated secretion directly.

Finally, the present results provide new information on the structure-function of family S1(clan SA) serine proteases.

Acknowledgement

This work was partly supported by grants from the Ministry of Education, Culture, Sports, Science, and Technology of Japan, and a research fellow ship of the Japan Society for the Promotion of Science in Japan.

I thank Dr. Sadao Siosaka (Division of structural cell biology, Nara Institute of Science and Technology (NAIST)) for help this study, Dr. Toshio Hakoshima (Division of structural biology, NAIST) for the critical review of neuropsin structural-function relationship, Dr. Masami Takahashi (Mitsubishi Kasei Institute of Life Sciences) for the suggestion on secretional analysis, and Dr. Keiko Kato (Division of structural cell biology, NAIST) for her devotional direction.

I am grateful to Ryoko Maesaki for her contribution to the development of schematic structure of neuropsin, Dr. Makoto Itakura for providing the useful hGH expression vector, Dr. Yasuhisa Fukui for providing PC12 cells, Saori Yamamori for her support my experiments, Dr. Kazumasa Matsumoto-miyai for providing recombinant neuropsin, Dr. Yasuhiko Horiguchi and Dr. Tamotsu Yoshimori for critical reading of the manuscript.

Those who most deserve my thanks are my family and my colleagues at NAIST.

References

1. Baranes, D., Lederfein, D., Huang, Y.-Y., Chen, M., Bailey, C. H., and Kandel, E. R. (1998). Tissue plasminogen activator contributes to the late phase of LTP and to synaptic growth in the hippocampal mossy fiber pathway. *Neuron* **21,** 813-825.

2. Komai, S., Matsuyama, T., Matsumoto, K., Kato, K., Kobayashi, M., Imamura, K., Yoshida, S., Ugawa, S., and Shiosaka, S. (2000). Neuropsin regulates an early phase of schaffer-collateral long-term potentiation in the murine hippocampus. *Eur. J. Neurosci.* **12,** 1479-1486.

3. Davies, B., Kearns, I. R., Ure, J., Davies, C. H., and Lathe, R. (2001). Loss of hippocampal serine protease BSP1/Neuropsin predisposes to global seizure activity. *J. Neurosci.* **21,** 6993-7000.

4. Nakagami, Y., Abe, K., Nishiyama, N., and Matsuki, N. (2000). Laminin degradation by plasmin regulates long-term potentiation. *J. Neurosci.* **20,** 2003-2010.

5. Nicole, O., Docagne, F., Ali, C., Margaill, I., Carmeliet, P., MacKenzie, E. T., Vivien, D., and Buisson, A. (2001). The proteolytic activity of tissue-plasminogen activator enhances NMDA receptor-mediated signaling. *Nat. Med.* **7,** 59-64.

6. Chen, Z.-L., Yoshida, S., Kato, K., Momota, Y., Suzuki, J., Tanaka, T., Ito, J., Nishino, H., Aimoto, S., Kiyama, H., and Shiosaka, S. (1995). Expression and activity-dependent changes of a novel limbic-serine protease gene in the hippocampus. *J. Neurosci.* **15,** 5088-5097.

7. Momota, Y., Yoshida, S., Ito, J., Shibata, M., Kato, K., Sakurai, K., Matsumoto, K., and Shiosaka, S. (1998). Blockade of neuropsin, a serine protease, ameliorates kindling epilepsy. *Eur. J. Neurosci.* **10**, 760-764.

8. Kato, K., Kishi, T., Kamachi, T., Akisada, M., Oka, T., Midorikawa, R., Takio, K., Dohmae, N., Bird, P. I., Sun, J., Scott, F., Miyake, Y., Yamamoto, K., Machida, A., Tanaka, T., Matsumoto, K., Shibata, M., and Shiosaka, S. (2001). Serine proteinase inhibitor 3 and murinoglobulin I are potent inhibitors of neuropsin in adult mouse brain. *J. Biol. Chem.* **276,** 14562-14571.

9. Suzuki, J., Yoshida, S., Chen, Z-L., Momota, Y., Kato, K., Hirata, A. and Shiosaka, S. (1995). Ontogeny of neuropsin mRNA expression in the mouse brain, *Neurosci. Res.* **23,** 345-351.

10. Kishi, T., Kato, M., Shimizu, T., Kato, K., Matsumoto, K., Yoshida, S., Shiosaka, S., and Hakoshima, T. (1999). Crystal structure of neuropsin, a hippocampal protease involved in kindling epileptogenesis. *J. Biol. Chem.* **274,** 4220-4224.

11. Barrett, A. J., Rawlings, N. D., and Woessner, J. F. (eds) (1998) in Handbook of Proteolytic Enzymes (Academic Press, UK) pp5-283.

12. Hedstrom, L., Szilagyi, L., and Rutter, W. J. (1992). Converting trypsin to Chymotrypsin: The role of surface loops. *Science* **255,** 1249-1253.

13. Perona, J. J., and Craik, C. S. (1995). Structural basis of substrate specificity in the serine proteases. *Protein Sci.* **4,** 337-360.

14. Perona, J. J., and Craik, C. S. (1997). Evolutionary divergence of substrate specificity within the chymotrypsin-like serine protease fold. *J. Biol. Chem.* **272,** 29987-29990.

15. Huang, C., Li, L., Krilis, S. A., Chanasyk, K., Tang, Y., Li, Z., Hunt, J. E., and Stevens, R. L. (1999). Human tryptases α and β/II are functionally distinct due, in part, to a single amino acid difference in one of the surface loops that forms the substrate-binding cleft. *J. Biol. Chem.* **274,** 19670-19676.

16. Bode, W., Turk, D., and Karshikov, A. (1992). The refined 1.9-A X-ray crystal structure of D-Phe-Pro-Arg chloromethylketone-inhibited human α-thrombin: Structure analysis, overall structure, electrostatic properties, detailed active-site geometry, and structure-function relationships. *Protein Sci.* **1,** 426-471.

17. Renatus, M., Engh, R. A., Stubbs, M. T., Huber, R., Fischer, S., Kohnert, U., and Bode, W. (1997). Lysine 156 promotes the anomalous proenzyme activity of tPA: X-ray crystal structure of single-chain human tPA. *EMBO J.* **16,** 4797-4805.

18. Takahashi, N., Tsukamoto, Y., Shiosaka, S., Kishi, T., Hakoshima, T., Arata, Y., Yamaguchi, Y., Kato, K., and Shimada, I. (1999). N-glycan structures of murine hippocampus serine protease, neuropsin, produced in *Trichoplusia ni* cells. *Glycoconj. J.* **16,** 405-414.

19. Bartunik, H. D., Summers, L. J., and Bartsch, H. H. (1989). Crystal structure of bovine β-trypsin at 1.5 A resolution in a crystal form with low molecular packing density. *J. Mol. Biol.* **210,** 813-828.

20. Bax, B., Blundell, T. L., Murray-Rust, J., and McDonald, N. Q. (1997).

Structure of mouse 7S NGF: a complex of nerve growth factor with four binding proteins. *Structure* **5,** 1275-1285.

21. Burgess, T. L., Craik, C. S., Matsuuchi, L., and Kelly, R. B. (1987). In vitro mutagenesis of trypsinogen: Role of the amino terminus in intracellular protein targeting to secretory granules. *J. Cell. Biol.* **105,** 659-668.

22. Gullberg, U., Lindmark, A., Lindgren, G., Persson, A.-M., Nilsson, E., and Olsson, I. (1995). Carboxyl-terminal prodomain-deleted human leukocyte elastase and cathepsin G are efficiently targeted to granules and enzymatically activated in the rat basophilic/mast cell line RBL. *J. Biol. Chem.* **270,** 12912-12918.

23. Parmer, R. J., Mahata, M., Mahata, S., Sebald, M. T., O'Connor, D. T., and Miles, L. A. (1997). Tissue plasminogen activator (t-PA) is targeted to the regulated secretory pathway. *J. Biol. Chem.* **272,** 1976-1982.

24. Garwicz, D., Lindmark, A., Persson, A.-M., and Gullberg, U. (1998). On the role of the proform-conformation for processing and intracellular sorting of human cathepsin G. *Blood* **92,** 1415-1422.

25. Sawyer, N., Rondeau, N., Chrétien, M., and Seidah, N. G. (1991). Expression and sorting of rat plasma kallikrein in POMC-producing AtT-20 cells. *DNA Cell. Biol.* **10,** 259-269.

26. Peters, J., Takahashi, S., Tada, M., and Miyake, Y. (1992). mGK-6-derived true tissue kallikrein is synthesized, processed, and targeted through a regulated secretory pathway in mouse pituitary AtT-20 cells. *J. Biochem.* **111,** 643-648.

27. Goslin, K. and Banker, G., Rat hippocampal neurons in low-density culture. In: G. Banker and K. Goslin (Eds.), Culturing Nerve Cells. MIT Press, Cambridge, MA, 1991, pp. 251-281.

28. Shimizu, C., Yoshida, S., Shibata, M., Kato, K., Momota, Y., Matsumoto, K., Shiosaka, T., Midorikawa, R., Kamachi, T., Kawabe, A., and Shiosaka, S. (1998). Characterization of recombinant and brain neuropsin, a plasticity-related serine protease. *J. Biol. Chem.* **273,** 11189-11196.

29. Niwa, H., Yamamura, K., and Miyazaki, J. (1991). Efficient selection for high-expression transfectants with a novel eukaryotic vector. *Gene* **108,** 193-200.

30. Mizuguchi, H., Nakagawa, T., Nakanishi, M., Imazu, S., Nakagawa, S., and

Mayumi, T. (1996). Efficient gene transfer into mammalian cells using fusogenic liposome. *Biochem. Biophys. Res. Commun.* **218,** 402-407.

31. Itakura, M., Misawa, H., Sekiguchi, M., Takahashi, S., and Takahashi, M. (1999). Transfection analysis of functional roles of complexin I and II in the exocytosis of two different types of secretory vesicles. *Biochem. Biophys. Res. Commun.* **265,** 691-696.

32. Matus, A., Bernhardt, R., Bodmer, R. and Alaimo, D. (1986). Microtubule-associated protein 2 and tubulin are differently distributed in the dendrites of developing neurons. *Neuroscience.* **17,** 371-389.

33. Huovila, A.-P. J., Eder, A. M., and Fuller, S. D. (1992). Hepatitis B surface antigen assembles in a post-ER, Pre-golgi compartment. *J. Cell. Biol.* **118,** 1305-1320.

34. Moremen, K. W. and Robbins, P. W. (1991). Isolation, characterization, and expression of cDNAs encoding murine α-mannosidase II, a golgi enzyme that controls conversion of high mannose to complex N-Glycans. *J. Cell. Biol.* **115,** 1521-1534.

35. Yoo, S. H. and Lim, D. J. (1993). Ubiquitous presence of chromogranin A in the inner ear of guinea pig. *FEBS lett.* **317,** 113-117.

36. Kim, T., Tao-Cheng, J.-H., Eiden, L. E., and Loh, Y. P. (2001). Chromogranin A, an "on/off" switch controlling dense-core secretory granule biogenesis. *Cell* **106,** 499-509.

37. Harlow, E. and Lane, D. (eds) (1988) in Antibodies: A Laboratory Manual (Cold Spring Harbor Laboratory, Cold Spring Harbor, NY.) pp418

38. Okabe, A., Tawara, Y., Masa, T., Oka, T., Machida, A., Tanaka, T., Matsuhashi, H., Shiosaka, S. and Kato, K. (2001). Differential expression of mRNAs for sialyltransferase isoenzymes induced in the hippocampus of mouse following kindled seizures. *J. Neurochem.* **77,** 1185-1197.

39. Fernandez, C. J., Haugwitz, M., Eaton, B., and Moore, H.-P. H. (1997). Distinct molecular events during secretory granule biogenesis revealed by sensitivities to brefeldin A. *Mol. Bio. Cell.* **8,** 2171-2185.

40. Cowley, D. J., Moore, Y. R., Darling, D. S., Joyce, P. B. M., and Gorr, S.-U. (2000). N- and C-terminal domains direct cell type-specific sorting of chromogranin A to secretory granules. *J. Biol. Chem.* **275,** 7743-7748.

41. Wick, P. F., Senter, R. A., Parsels, L. A., Uhler, M. D., and Holz, R. W. (1993) Transient transfection studies of secretion in bovine chromaffin cells and PC12 cells. *J. Biol. Chem.* **268,** 10983-10989.

42. Shiosaka, S. and Yoshida, S. (2000). Synaptic microenvironments–structural plasticity, adhesion molecules, proteases and their inhibitors. *Neurosci. Res.* **37,** 85-89.

43. Treubert, U. and Brüm mendorf, T. (1998). Functional cooperation of β1-integrins and members of the Ig superfamily in neurite outgrowth induction. *J. Neurosci.* **18,** 1795-1805.

44. Stallcup, W.B. and Beasley, L. (1985). Involvement of the nerve growth factor-inducible large external glycoprotein (NILE) in neurite fasciculation in primary cultures of rat brain. *Proc. Natl. Acad. Sci. U. S. A.* **82,** 1276-1280.

45. Lagenaur, C. and Lemmon, V. (1987). An L1-like molecule, the 8D9 antigen, is a potent substrate for neurite extension. *Proc. Natl. Acad. Sci. U. S. A.* **84,** 7753-7757.

46. Schmid, R.-S., Pruitt, W.M. and Maness, P.F. (2000). A MAP kinase-signaling pathway mediates neurite outgrowth on L1 and requires Src-dependent endocytosis. *J. Neurosci.* **20,** 4177-4188.

47. Gutwein, P., Oleszewski, M., Mechtersheimer, S., Agmon-Levin, N., Krauss, K. and Altevogt, P. (2000). Role of src kinases in the ADAM-mediated release of L1 adhesion molecule from human tumor cells. *J. Biol. Chem.* **275,** 15490-15497.

48. Yi, M. and Ruoslahti, E. (2001). A fibronectin fragment inhibits tumor growth, angiogenesis, and metastasis. *Proc. Natl. Acad. Sci. U. S. A.* **98,** 620-624.

49. Liljelund, P., Ghosh, P. and van den Pol, A. N. (1994). Expression of the neural axon adhesion molecule L1 in the developing and adult rat brain. *J. Biol. Chem.* **269,** 32886-32895.

50. Willett, W. S., Gillmor, S. A., Perona, J. J., Fletterick, R. J., and Craik, C. S. (1995). Engineered metal regulation of trypsin specificity. *Biochemistry* **34,** 2172-2180.

51. Gabel, D. and Kasche, V. (1973). Autolysis of β-trypsin. *Acta Chem. Scand.* **27,** 1971-1981.

52. Brechler, V., Chu, W. N., Baxter, J. D., Thibault, G., and Reudelhuber, T. L.

(1996). A protease processing site is essential for prorenin sorting to the regulated secretory pathway. *J. Biol. Chem.* **271,** 20636-20640.

53. Cool, D. R., Fenger, M., Snell, C. R., and Loh, Y. P., (1995). Identification of the sorting signal motif within pro-opiomelanocrtin for the regulated secretory pathway. *J. Biol. Chem.* **270,** 8723-8729.

54. Creemers, J. W. M., Usac, E. F., Bright, N. A., Van de Loo, J.-W., Jansen, E., Van de Ven, W. J. M., and Hutton J. C. (1996). Identification of a transferable sorting domain for the regulated pathway in the prohormone convertase PC2. *J. Biol. Chem.* **271,** 25284-25291.

55. Zhang, C.-F., Snell, C. R., and Loh, Y. P., (1999). Identification of a novel prohormone sorting signal-binding site on carboxypeptidase E, a regulated secretory pathway-sorting receptor. *Mol. Endocrinol.* **13,** 527-536.

56. Zhou, A., Webb, G., Zhu, X., and Steiner, D. F. (1999). Proteolytic processing in the secretory pathway. *J. Biol. Chem.* **274,** 20745-20748.

57. Jutras, I., Seidah, N. G., and Reudelhuber, T. L. (2000). A predicted α-helix mediates targeting of the proprotein convertase PC1 to the regulated secretory pathway. *J. Biol. Chem.* **275,** 40337-40343.

58. Mouchantaf, R., Kumar, U., Sulea, T., and Patel, Y. C. (2001). A conserved α-helix at the amino terminus of prosomatostatin serves as a sorting signal for the regulated secretory pathway. *J. Biol. Chem.* **276,** 26308-26316.

59. Matzuk, M. M., and Boime, I. (1988). The role of the asparagine-linked oligosaccharides of the α subunit in the secretion and assembly of human chorionic gonadotropin. *J. Cell. Biol.* **106,** 1049-1059.

60. Shakin-Eshleman, S. H., Remaley, A. T., Eshleman, J. R., Wunner, W. H., and Spitalnik, S. L. (1992). *N*-linked glycosylation of rabies virus glycoprotein. *J. Biol. Chem.* **267,** 10690-10698.

61. Kitagawa, Y., Sano, Y., Ueda, M., Higashio, K., Narita, H., Okano, M., Matsumoto, S., and Sasaki, R. (1994). N-glycosylation of erythropoietin is critical for apical secretion by madin-darby canine kidney cells. *Exp. Cell. Res.* **213,** 449-457.

62. Haraguchi, M., Yamashiro, S., Furukawa, K., Takamiya, K., Shiku, H., and Furukawa, K. (1995). The effects of the site-directed removal of N-glycosylation sites

from β-1,4-*N*-acetylgalactosaminyltransferase on its function. *Biochem. J.* **312,** 273-280.

63. Letourneur, O., Sechi, S., Willette-Brown, J., Robertson, M. W., and Kinet, J.-P. (1995). Glycosylation of human truncated FcεRI α chain is necessary for efficient folding in the endoplasmic reticulum. *J. Biol. Chem.* **270,** 8249-8256.

64. Scheiffele, P., Peränen, J., and Simons, K. (1995). *N*-glycans as apical sorting signals epithelial cells. *Nature* **378,** 96-98.

65. Martina, J. A., Daniotti, J. L., and Maccioni, H. J. F. (1998). Influence of *N*-glycosylation and *N*-glycan trimming on the activity and intracellular traffic of GD3 synthase. *J. Biol. Chem.* **273,** 3725-3731.

66. Branza-Nichita, N., Negroiu, G., Petrescu, A. J., Garman, E. F., Platt, F. M., Wormald, M. R., Dwek, R. A., and Petrescu, S. M. (2000). Mutations at critical *N*-glycosylation sites reduce tyrosinase activity by altering folding and quality control. *J. Biol. Chem.* **275,** 8169-8175.

67. Kadowaki, T., Tsukuba, T., Bertenshaw, G. P., and Bond, J. S. (2000). *N*-linked oligosaccharides on the Meprin A metalloprotease are important for secretion and enzymatic activity, but not for apical targeting. *J. Biol. Chem.* **275,** 25577-25584.